Journal of Natural Gas Science and Engineering 45 (2017) 797–811

Contents lists available at ScienceDirect

Journal of Natural Gas Science and Engineering

journal homepage: www.elsevier.com/locate/jngse

Numerical assessment of the influences of coal permeability and gas pressure inhomogeneous distributions on gas drainage optimization

Qingquan Liu [a, b, c, *], Yuanping Cheng [a, c, **], Haifeng Wang [a, c], Shengli Kong [d], Jun Dong [a, c], Mingyi Chen [a, c], Hao Zhang [a, c]

[a] Key Laboratory of Coal Methane and Fire Control, Ministry of Education, China University of Mining & Technology, Xuzhou 221116, China
[b] State Key Laboratory of Coal Resources and Safe Mining, China University of Mining & Technology, Beijing 100083, China
[c] National Engineering Research Center for Coal Gas Control, China University of Mining & Technology, Xuzhou 221116, China
[d] College of Urban Construction and Safety Engineering, Shanghai Institute of Technology, Shanghai 201418, China

ARTICLE INFO

Article history:
Received 6 November 2016
Received in revised form
3 June 2017
Accepted 6 July 2017
Available online 8 July 2017

Keywords:
Gas drainage
Reservior inhomogeneity
Gas migration
Numerical simulation
Image recognition

ABSTRACT

In this paper, significant effort was devoted to theoretical/numerical modeling to make an optimal gas drainage design for a pre-drainage coal seam considering the inhomogeneity of coal permeability and gas pressure. A fully coupled model of gas flow, gas diffusion and permeability evolution was developed to evaluate the borehole drainage performances of safety needs (primary consideration) and economic efficiency (secondary consideration). A novel method was applied to rebuilt the non-uniform initial condition in COMSOL to realize the inhomogeneous distribution of coal permeability and gas pressure in the numerical simulations. The significant influences of the inhomogeneity of coal permeability and gas pressure on gas drainage were discussed, and two main disadvantages were visually revealed, including unnecessary engineering cost and enormous mining risk. The optimal gas drainage design consists of three different borehole spacings available for 6 zones, being able to save about 21.5% engineering cost compared to that without considering the reservior inhomogeneity. Numerical simulation results are also helpful to the gas drainage technological innovations.

1. Introduction

Coal mine methane (CMM) is both a potentially valuable energy and a serious hazard in active coal mines, degassing coal seams is an important for mitigating this hazard and results in the beneficial recovery of a cleanburning, low-carbon fuel resource (Karacan et al., 2011). Shanxi province is the most important coal production base of China, and its landform characteristics are very special: the Loess Plateau and its dusty soil cover almost the whole Shanxi province, which has long been suffering from serious soil erosion, resulting in most parts of Shanxi province is gully-hill dominated (Zhao et al., 2013; Shi and Shao, 2000). The gully-hill dominated landform greatly influences the buried depth, generating typically inhomogeneous distributions of gas pressure and coal permeability, and further influences gas drainage.

The drainage performance of boreholes is the main foundation to make gas drainage design, which usually can only be pre-evaluated by numerical simulations based on strict theoretical modeling of the physical mechanism of gas drainage. Reservoir-simulation technology has the capability to provide us with an economical mean to solve complex engineering problems, the successful quantitative evaluations of gas drainage in a coal seam are not only based on the gas migration theory but also based on the valid predictions of gas occurrence distribution and coal permeability distribution.

A significant amount of work has been completed in the area of modeling gas diffusion, gas flow, coal permeability (coupled hydro-mechanical response) and FEM (finite element method) calculation (Wei et al., 2007; Manik et al., 2000).

According to the physical mechanism of gas drainage, the theoretical model should consist of the governing equations of gas flow, gas diffusion and permeability evolution, and the achievements of the coupling relations between the three field governing

* Corresponding author. Key Laboratory of Coal Methane and Fire Control, Ministry of Education, China University of Mining & Technology, Xuzhou 221116, China.
** Corresponding author. Key Laboratory of Coal Methane and Fire Control, Ministry of Education, China University of Mining & Technology, Xuzhou 221116, China.
E-mail addresses: cumtsafe@cumt.edu.cn (Q. Liu), ypcheng@cumt.edu.cn (Y. Cheng).

http://dx.doi.org/10.1016/j.jngse.2017.07.003
1875-5100/

equations. Valliappan and Zhang (1996) presented a coupling mathematical model for gas flow and coal deformation, and the diffusion effect of adsorbed methane has been taken into account. Gilman and Beckie (2000) pointed out that coal-seam methane reservoirs have some unique features compared to conventional gas reservoirs, and proposed a simplified mathematical model of methane migration in a coal seam taking these unique features into account. In consideration that many coals exhibit bi- or multimodal pore structure, Shi and Durucan (2003) developed a bidisperse pore model for gas diffusion in coal matrix. Ye et al. (2014). studied the non-Darcy flow behavior in coal seams by coupling coal permeability change and variable non-Darcy factor in a dual porosity model. Zhu et al. (2011). built a fully coupled model to examine the complex coal-gas interactions under variable temperatures.

Moreover, in general, it is impossible to get a theoretical solution for the fully coupled model of gas flow, gas diffusion and permeability evolution, and numerical simulation is an effective method to the multi-physical phenomena. Based on a quasisteady-state, nonequilibrium diffusion-sorption model, King et al. (1986) developed a numerical model for the simulation of the unsteady-state flow of methane and water through dual-porosity coal seams. Manik et al. (2000). developed a three-dimensional, two-phase, dual porosity, fully implicit, coalbed compositional simulator. Clarkson et al (Clarkson and McGovern, 2005). presented a new coal-bed methane (CBM) prospecting tool by combining single-well reservoir simulators with a gridded reservoir model, Monte Carlo simulation, and economic modules. Thararoop et al. (2012). developed a multi-mechanistic, dual-porosity, dual-permeability, numerical flow model for CBM reservoirs, taking the effects of water presence in the coal matrix into account. Chen et al. (2013) improved an relative permeability model for coal reservoirs, which was then coupled into the reservoir simulation model to study how the coal porosity change induced relative permeability change affects the CBM production. Wei et al. (2007). reviewed three types of existing CBM reservoir models, including conventional black-oil and compositional models, specialized CBM models and improved CBM models. Liu and Cheng (2014) conducted a series of numerical simulations and field tests to study the influences of pressure drop on gas drainage. Yang et al. (2010). studied the dynamic process of pressure relief and gas drainage during coal mining by conducting a series of numerical simulations. Liu et al (Yanwei et al., 2016). studied the influence factors of high-pressure hydraulic flush enhanced gas drainage based on a numerical method.

Though the mechanism and numerical simulator of gas migration in a coal seam have drawn a lot of attention, most of the recently published studies are focused on CBM recovery. To some degree, the physical mechanism of gas drainage is similar to that of CBM extraction. However, the objectives of gas drainage and CBM extraction are different. The main objective of gas drainage (degassing coal seam) is to mitigate coal and gas outburst hazards. Comparing with CBM recovery, quantitative evaluations of gas drainage is more critical as which is closely related to the mining safety. Thus, gas drainage design is mainly based on the borehole drainage performance related to safety needs, instead of economic efficiency (which is the secondary consideration). Moreover, considering the safety needs of coal mines in Shanxi province, the inhomogeneous distributions of gas pressure and coal permeability (induced by the influences of the loess plateau geomorphology) should be taken into account when conducting the numerical simulation, which has seldom been implemented in numerical simulators of gas migration to date. Therefore, further efforts should be made to fill a gap in quantitative evaluations of gas drainage performance while ensuring that the influences of the inhomogeneous distributions of gas pressure and coal permeability are taken into account.

The primary objective of this paper is to make an optimal gas drainage design for a pre-drainage coal seam considering the inhomogeneous distributions of gas pressure and coal permeability. The principal feature of this work is that the influences of the inhomogeneous distributions of gas pressure and coal permeability on gas drainage are investigated through theoretical/numerical modeling. To achieve this goal, a fully coupled model of gas migration in a coal seam was developed; image recognition technology was applied to rebuilt the initial inhomogeneous condition in numerical simulators. By conducting two numerical case studies, disadvantages of drainage design without considering the inhomogeneous distributions of gas pressure and coal permeability and the optimal gas drainage design were analyzed. The numerical simulations are helpful to the gas drainage technological innovations.

2. Mathematical model

In the following, a set of governing equations are deduced which govern the gas diffusion, gas flow, coal deformation and dynamic permeability evolution. These derivations are based on several simplifying assumptions: (1) The coal seam is dry and isothermal, ignoring the influences of water and temperature. (2) The coal seam is an isotropic and dual poroelastic but inhomogeneous medium. (3) Methane behaves as an ideal gas, and its viscosity is constant under isothermal conditions. (4) Coal is saturated by methane.

Besides, to describe the storage state and migration of CMM in a coal seam, we utilize the dual porosity concept (Liu et al., 2015a). That is, the coal seam is typically dual-porosity systems that consist of coal matrix surrounded by intersecting fractures. In such a dual porosity medium, at every point, two pressures are defined: the pressure in fractures, p_f, and the pressure in coal matrix, p_m. Since one can hardly speak about the free gas (and gas pressure) in micropores, p_m is defined as the "virtual" pressure that would be in equilibrium with the current concentration of adsorbate in matrix blocks (Gilman and Beckie, 2000).

2.1. Gas release from the coal matrix

Gas release from the coal matrix is assumed to be driven by the concentration gradient, and the gas exchange rate can be expressed as (Mora and Wattenbarger, 2009; Wang et al., 2012)

$$Q_m = \frac{1}{\tau}\left(c_m - c_f\right) \tag{1}$$

where Q_m is the gas exchange rate per volume of coal matrix blocks, kg/(m^3·s). c_m is the concentration of gas in the matrix blocks, kg/m^3. c_f is the concentration of gas in the fractures, kg/m^3. τ represents the "sorption time", and it is numerically equivalent to the time during which 63.2% of the coal gas content is desorbed (Mora and Wattenbarger, 2009; An et al., 2013; Zuber et al., 1987), s; Moreover, it has a reciprocal relationship with the diffusion coefficient and shape factor $\tau = 1/(D \cdot \sigma_c)$, where D is the gas diffusion coefficient, m^2/s; σ_c is coal matrix block shape factor, m^{-2}.

Based on the assumptions and make use of the ideal gas law:

$$c_m = \frac{M_c}{RT} p_m \tag{2}$$

$$c_f = \frac{M_c}{RT} p_f \tag{3}$$

where M_c is the molar mass of methane, kg/mol. R is the universal gas constant, J/(mol·K). T is the temperature, K.

By applying the mass conservation law to the coal matrix, we have

$$\frac{\partial m}{\partial t} = -Q_m \tag{4}$$

where t is time, s. m is the quantity of adsorbed gas and free gas per volume of coal matrix blocks, kg/m^3, which can be calculated using the Langmuir equation and the ideal gas law:

$$m = \frac{V_L p_m}{p_m + P_L}\frac{M_c}{V_M}\rho_c + \phi_m \frac{M_c}{RT} p_m \tag{5}$$

where V_L denotes the maximum adsorption capacity of the coal, m^3/kg. P_L denotes the Langmuir pressure constant, Pa. V_M is the molar volume of methane under standard conditions, m^3/mol. ρ_c is the coal density, kg/m^3. ϕ_m is the coal matrix porosity, %.

By substituting Eqs. (1)–(3) and (5) into Eq. (4), we obtain the governing equation for the gas pressure change in the coal matrix blocks:

$$\frac{\partial p_m}{\partial t} = -\frac{V_M\left(p_m - p_f\right)(p_m + P_L)^2}{\tau V_L R T P_L \rho_c + \tau \phi_m V_M (p_m + P_L)^2} \tag{6}$$

2.2. Balance equations and flow in fractures

The transfer of free gas through the fractures in a coal seam is governed by a mass conservation equation (Hassanizadeh, 1986):

$$\frac{\partial}{\partial t}\left(\phi_f \rho_g\right) = -\nabla\left(\rho_g V\right) + Q_m \tag{7}$$

where ϕ_f is the fracture porosity, %. ρ_g is the gas density, kg/m^3, and $\rho_g = M_c p_f / RT$. V is the gas velocity in fractures, m/s.

Volumetric flow in the fractures is governed by Darcy's law, we have

$$V = -\frac{k}{\mu}\nabla p_f \tag{8}$$

where k is coal permeability, mD. μ is the methane viscosity, Pa·s.

By substituting Eqs. (1) and (8) into Eq. (7), we obtain the governing equation for the gas pressure change in the fractures:

$$\phi_f \frac{\partial p_f}{\partial t} + p_f \frac{\partial \phi_f}{\partial t} = \nabla\left(\frac{k}{\mu} p_f \nabla p_f\right) + \frac{1}{\tau}\left(p_m - p_f\right) \tag{9}$$

2.3. Governing equation for coal deformation

The presence of methane in coal modifies its mechanical response, and in turn, the change of coal mechanical response will affect the migration of methane. Considering the characteristics of a dual-porosity medium and differences between p_f and p_m, the dual poroelasticity theory is used to define the volumetric response of coal induced by gas pressure change.

For a dual-porosity medium, the effective stress can be calculated by (Mian and Zhida, 1999; Zhang et al., 2004)

$$\sigma_{ij}^e = \sigma_{ij} - \left(\beta_f p_f + \beta_m p_m\right)\delta_{ij} \tag{10}$$

where σ_{ij}^e is the effective stress, MPa. σ_{ij} is the total stress (positive in compression), MPa. δ_{ij} is the Kronecker delta tensor. $\beta_f = 1 - K/K_m$ and $\beta_m = K/K_m - K/K_s$, where K is the bulk modulus of coal, and $K = E/3(1-2\upsilon)$, MPa; K_m is the bulk modulus of the coal grains, and $K_m = E_m/3(1-2\upsilon)$, MPa; K_s is the bulk modulus of the coal skeleton, and $K_s = K_m/[1 - 1.5\phi_m(1-\upsilon)/(1-2\upsilon)]$, MPa; β_f and β_m are effective stress coefficients for fractures and coal matrix blocks, respectively E is the Young's modulus of the coal, MPa. E_m is the Young's modulus of the coal grains, MPa. υ is the Poisson's ratio of the coal.

The strain-displacement relationship is defined as:

$$\varepsilon_{ij} = \frac{1}{2}\left(u_{i,j} + u_{j,i}\right) \tag{11}$$

where ε_{ij} denotes the component of the total strain tensor. u_i denotes the displacement component in the i-direction.

The equilibrium equation is defined as

$$\sigma_{ij,j} + F_i = 0 \tag{12}$$

where F_i denotes the body force component in the i-direction.

Based on the dual-poroelastic theory, the constitutive relation for the coal seam can be expressed as (Detournay and Cheng, 1993):

$$\varepsilon_{ij} = \frac{1}{2G}\sigma_{ij} - \left(\frac{1}{6G} - \frac{1}{9K}\right)\sigma_v \delta_{ij} + \frac{1}{3K}\beta_f p_f \delta_{ij} + \frac{1}{3K}\beta_m p_m \delta_{ij} + \frac{\varepsilon_s}{3}\delta_{ij} \tag{13}$$

where G is the shear modulus of coal, and $G = E/2(1+\upsilon)$, MPa. $\sigma_v = \sigma_{11} + \sigma_{22} + \sigma_{33}$. ε_s is the sorption-induced volumetric strain, and can be calculated by a Langmuir-type equation

$$\varepsilon_s = \varepsilon_L \frac{p_m}{P_L + p_m} \tag{14}$$

where ε_L is the Langmuir volumetric strain. The volumetric strain of the coal can be calculated by

$$\varepsilon_v = \varepsilon_{11} + \varepsilon_{22} + \varepsilon_{33} = \frac{1}{3K}\sigma_v + \frac{\beta_f}{K} p_f + \frac{\beta_m}{K} p_m + \varepsilon_s \tag{15}$$

Combining Eqs. 11–13 yields the Navier-type equation for coal seam deformation:

$$G u_{i,jj} + \frac{G}{1-2\upsilon} u_{j,ji} - \beta_f p_{f,i} - \beta_m p_{m,i} - K\varepsilon_{s,i} + F_i = 0 \tag{16}$$

2.4. Dynamic permeability model for fractures

The permeability of coal is a function of its fracture system, and the relationship between fracture porosity and permeability can be defined as:

$$\frac{k}{k_0} = \left(\frac{\phi_f}{\phi_{f0}}\right)^3 \tag{17}$$

where k_0 is the initial coal permeability, mD. ϕ_{f0} is the initial fracture porosity, %.

Under uniaxial strain conditions (expected in CBM reservoirs), coal deformation induced by gas pressures change is small, i.e.,

belongs to elastic deformation. Therefore, the relationship between fracture porosity, coal volumetric strain, grain volumetric strain and pore volumetric strain can be determined by the poroelastic theory as (Palmer and Mansoori, 1996)

$$d\varepsilon_p = \frac{d\varepsilon_v}{\phi_f} - \left(\frac{1-\phi_f}{\phi_f}\right)d\varepsilon_g \tag{18}$$

where ε_p is the pore volumetric strain. ε_g is the grain volumetric strain. Eq. (18) shows that the change of pore volume strain ε_p is a result of the coal volumetric strain and grain volumetric strain which are controlled by the competing influences of effective stress and sorption-induced volume change (as defined by Eq. (15)). Moreover, according to the dual poroelasticity theory, the volumetric response of coal induced by gas pressure change can be defined as (Liu et al., 2015a; Detournay and Cheng, 1993)

$$d\phi_f\left(p_f, p_m\right) = \frac{\beta_f}{M}dp_f + \left[\frac{\beta_m}{M} + \left(\frac{K}{M}-1\right)\frac{d}{dp_m}\left(\frac{\varepsilon_L p_m}{p_m + P_L}\right)\right]dp_m \tag{19}$$

where M is the constrained axial modulus, and $M = E(1-\upsilon)/[(1+\upsilon)(1-2\upsilon)]$, MPa.

Eq. (19) is a total differential form equation and its solution is easy to obtain based on the theory of multivariable differential calculus (Kriz and Pultr, 2013)

$$\frac{\phi_f}{\phi_{f0}} = 1 + \frac{1}{M\phi_{f0}}\left[\beta_f\left(p_f - p_{f0}\right) + \beta_m(p_m - p_{m0})\right] + \frac{\varepsilon_L}{\phi_{f0}}\left(\frac{K}{M}-1\right)\left(\frac{p_m}{P_L + p_m} - \frac{p_{m0}}{P_L + p_{m0}}\right) \tag{20}$$

where p_{f0} and p_{m0} are the initial gas pressures in coal fractures and coal matrix, MPa, and p_{f0} equals to p_{m0} when the initial state is an adsorption equilibrium state. The partial derivative of ϕ_f with respect to time, which is needed in Eq. (7), can be obtained from Eq. (20):

$$\frac{\partial\phi_f\left(p_f, p_m\right)}{\partial t} = \frac{1}{M}\left(\beta_f\frac{\partial p_f}{\partial t} + \beta_m\frac{\partial p_m}{\partial t}\right) + \frac{\varepsilon_L P_L}{(P_L + p_m)^2}\left(\frac{K}{M}-1\right)\frac{\partial p_m}{\partial t} \tag{21}$$

The resulting dynamic permeability model, derived from Eq. (17) and Eq. (20), takes the form

$$k = k_0\left\{1 + \frac{1}{M\phi_{f0}}\left[\beta_f\left(p_f - p_{f0}\right) + \beta_m(p_m - p_{m0})\right] + \frac{\varepsilon_L}{\phi_{f0}}\left(\frac{K}{M}-1\right)\left(\frac{p_m}{P_L + p_m} - \frac{p_{m0}}{P_L + p_{m0}}\right)\right\}^3 \tag{22}$$

2.5. Initial and boundary conditions

For completeness, the standard boundary and initial conditions are defined. The Dirichlet and Neumann boundary conditions for the gas diffuse (Eq. (6)), and gas flow (Eq. (9)) process are defined as

$$\text{Dirichlet boundary condition}: \ p_m = p_f = p_c \text{ on } \partial\Omega \tag{23}$$

$$\text{Neumann boundary condition}: \ \nabla p_m \cdot \vec{n} = 0, \ \nabla p_f \cdot \vec{n} = 0 \text{ on } \partial\Omega \tag{24}$$

where p_c is the given constant pressure on the boundaries, MPa. $\vec{n}$ is the outward unit normal vector on the boundary. Ω represents the subdomain on which the balances are performed. $\partial\Omega$ represents the boundaries of the subdomain. The Neumann boundary condition is also known as the no-flow boundary condition.

The initial condition for gas diffuse, and gas flow is

$$p_{f0} = p_{m0} = p_0 \text{ in } \Omega \tag{25}$$

The displacement and stress conditions on the boundaries for the Navier equation, Eq. (16), are given as

$$u_i = u_i(t) \text{ on } \partial\Omega \tag{26}$$

$$\sigma_{ij}\vec{n} = f_i(t) \text{ on } \partial\Omega \tag{27}$$

where $u_i(t)$ and $f_i(t)$ are the given displacement and stress on the boundary, respectively.

The initial conditions for displacement and stress are

$$u_i(0) = u_0 \text{ in } \Omega \tag{28}$$

$$\sigma_{ij}(0) = \sigma_o \text{ in } \Omega \tag{29}$$

where u_0 and σ_o are the initial values of displacement and stress and gas pressure in the domain.

3. Numerical simulation method

3.1. Finite element implementation in COMSOL

Eqs. (1), (6), (9), (21) and (22), incorporating the initial and boundary conditions define a theoretical model of coupled gas migration and permeability evolution of a coal seam. These field equations for gas migration and permeability evolution form a typical fluid dynamics problem, involving fully coupled, second order partial differential equations (PDE) whose nonlinearity appears in both space and time domains. Thus, it is difficult to obtain a theoretical solution for these partial differential equations.

In this work, the field equations with the boundary conditions were solved numerically using COMSOL Multiphysics software which has been proved to have professional facilities to solve multiphysics coupled problem based on the finite element method (FEM) (Shirazian et al., 2012; Liu et al., 2014, 2015b). In detail, Eq. (6) which is the field equation of gas release from the coal matrix was imported in the “PDE module”; Eq. (9) which is the field equation of gas flow in fractures was imported in the “Darcy's Law module”; Eqs. (1), (21) and (22) were imported as variables to define mass transfer between fractures and coal matrix, and evolutions of fracture porosity and coal permeability, respectively. In doing so, the developed theoretical model can be well solved.

3.2. Numerical model description and input parameters

To investigate a reasonable gas drainage design considering the influences of the inhomogeneous distributions of gas pressure and coal permeability, a simulation model was constructed based on the engineering background and some essential simplifications. Hexi coal mine is located in Liulin County (western region of Shanxi province) which is characterized by typical loess plateau geomorphology. The length and width of the pre-drainage coal seam are about 400 m and 1600 m, respectively. As shown in Fig. 1, for the pre-drainage area, the buried depth ranges between 349 m and 479 m, the gas pressure ranges between 0.81 MPa and 1.66 MPa, and coal permeability ranges between 0.0137 mD and 0.0508 mD, forming quite inhomogeneous initial distributions of gas pressure and coal permeability.

To import the inhomogeneous distributions of buried depth, gas pressure and coal permeability into COMSOL, the image recognition technology was applied. It is well known that the RGB color model had been widely used in sensing, representation and display of images in electronic systems. The image recognition was achieved by scaling the RGB values in each pixel. Then, we can rebuild the image in COMSOL based on the scaled the RGB values.

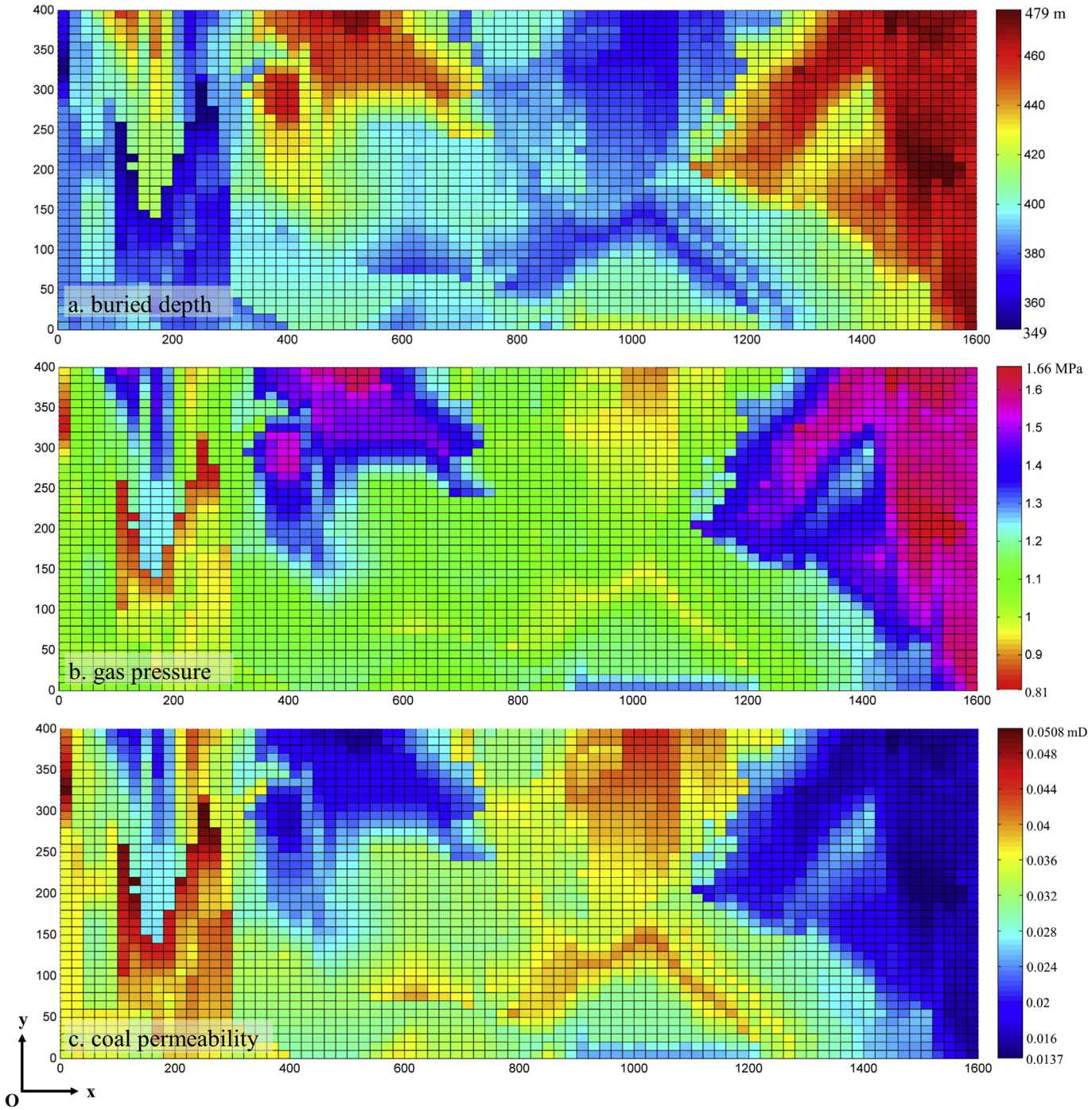

Fig. 1. Inhomogeneous initial distributions of buried depth, gas pressure and coal permeability.

As shown in Fig. 2, the upper image represents the statistics of the buried depth distribution, and the lower image represents the recognized data. The recognized image has the same size with the study area, i.e., 400 × 1600 m, and we use the function im1 (x, y) to load data from the recognized image in COMSOL (Multiphysics, 2015). As the recognized image is far bigger than the original image of buried depth, a linear interpolation method was used to realize the image zoom in, resulting in the recognized image is somewhat fuzzier than the original image. Moreover, color and data range of the original image is between 349 and 479, which of the recognized image is between 0.02 and 1. Thus, color and data range transformation of the recognized image should be made:

$$H = \frac{130}{0.98} \times [im1(x,y) - 0.02] + 349 \tag{30}$$

where H is the buried depth, m. $im1(x,y)$ is the recognized value at point (x,y) loaded from the recognized image. The inhomogeneous distributions of gas pressure and coal permeability can be imported into COMSOL by the similar operations to the buried depth.

The geometry and boundary conditions of the numerical model are shown in Fig. 3. The 2D solution domain measures 1600 m across by 400 m in length as the geometric model is a simplification of the pre-drainage area coal seam. The average thickness of pre-drainage area coal seam is 1.91 m and is quite smaller comparing with the length. Thus, the 2D geometric model was built to simplify the calculation. A series of methane drainage boreholes were set in the solution domain, whose length and radius were 400 m and 154 mm, respectively. In particular, as the sealing length of a borehole is usually shorter than 20 m in engineering, i.e. far shorter than the borehole. To avoid the negative influence of sealing part in a borehole on the finite element mesh generation, the sealing part has not been taken into account in building the geometry model.

Suitable boundary conditions were applied to the numerical model based on the theory presented in Section 2.5. A constant pressure of atmospheric pressure was applied to the top boundary, and a constant pressure of 87 kPa (less than atmospheric pressure) was applied to methane drainage boreholes, while no flow conditions were applied to the other three boundaries.

The initial pressure and initial permeability applied to the numerical model were also based on the case conditions. The influences of the inhomogeneous distributions of gas pressure and coal permeability on gas drainage were analyzed by conducting two case studies:

Case A was conducted to study disadvantages of drainage design without considering the influences of the inhomogeneous distributions of gas pressure and coal permeability. In this case study, the spacing of boreholes was obtained without considering the inhomogeneous initial gas pressure and coal permeability distributions, i.e., the initial gas pressure and initial coal permeability were uniform. The two key parameters were obtained by the field tests, and whose values are 1.58 MPa and 0.01565 mD respectively. Then, the corresponding disadvantages were analyzed by comparing the gas pressure distribution with that considering the inhomogeneous initial gas pressure and coal permeability (obtained by the image recognition technology).

Case B was conducted to study how to make gas drainage design

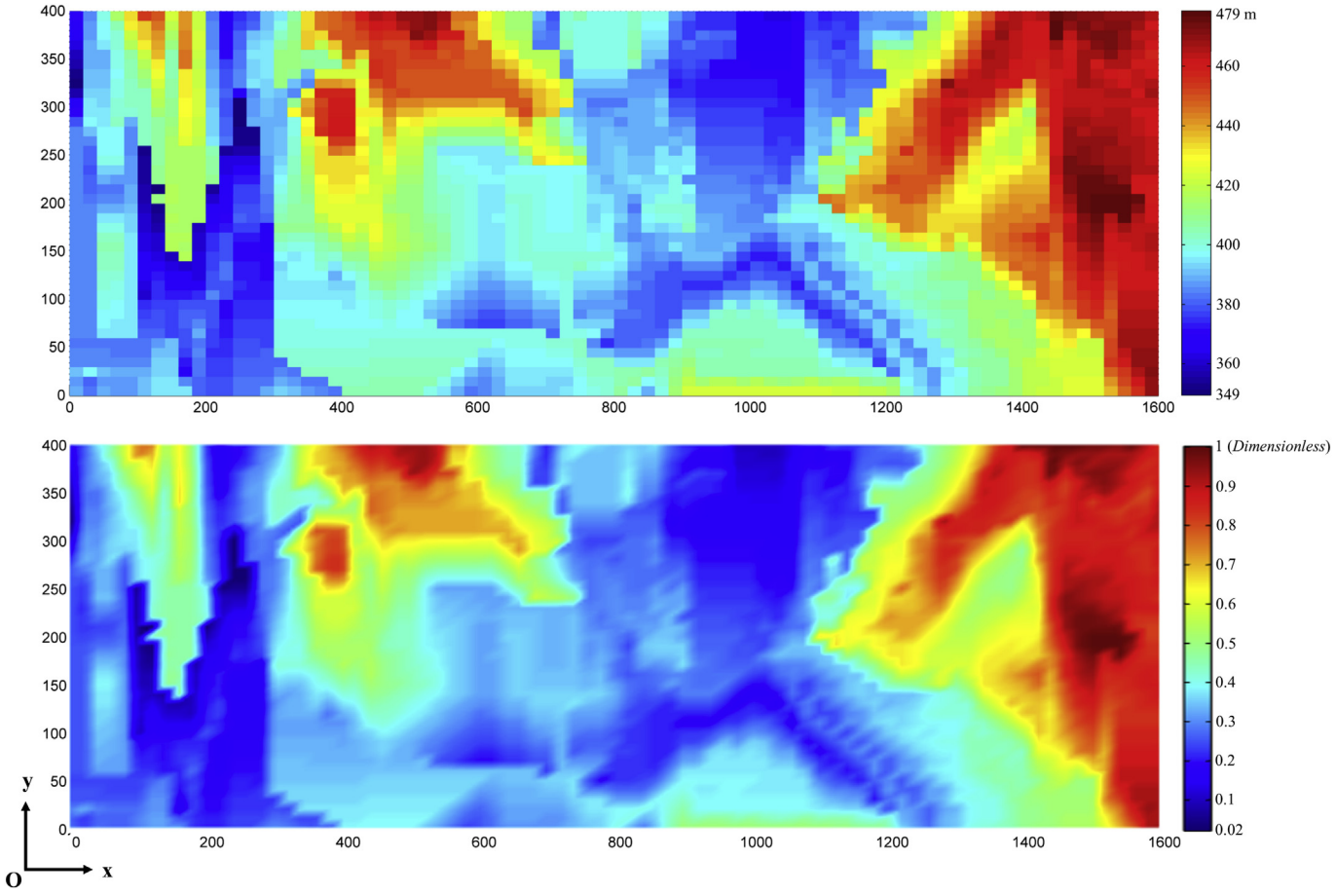

Fig. 2. Comparison of the statistical buried depth distribution and the recognized distribution.

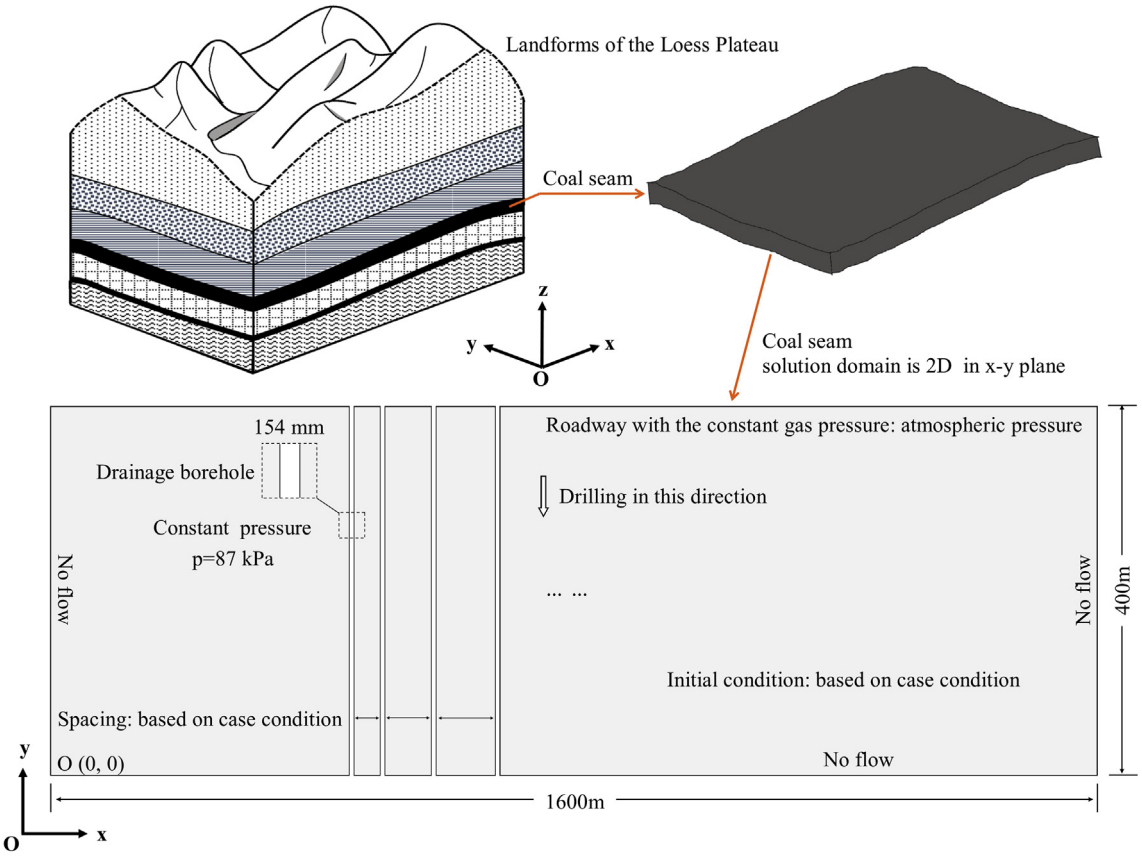

Fig. 3. Geometry and boundary conditions for gas drainage of the studied coal seam.

Table 1
Property parameters used in the simulation model.

Parameter	Value
Young's modulus of coal, E (MPa)	822
Poisson's ratio of coal, υ	0.25
Young's modulus of coal grains, E_m (MPa)	2466
Initial fracture porosity of coal, ϕ_{f0}	0.008
Initial porosity of coal matrix, ϕ_{m0}	0.059
Langmuir pressure constant, P_L (MPa)	1.67
Langmuir volume constant, V_L (m^3/t)	21.5
Sorption time, τ (d)	10
Langmuir volumetric strain constant, ε_L	0.01952
Density of coal, ρ_c (kg/m^3)	1250
Molar mass of methane, M_c (kg/mol)	0.016
Temperature, T (K)	293
Gas viscosity, μ (Pa·s)	1.84×10^{-5}
Drainage time, t (d)	600

with considering the influences of the inhomogeneous distributions of gas pressure and coal permeability. The initial gas pressure and initial coal permeability were applied as image recognized values of gas pressure and coal permeability.

For a more accurate evaluation of the gas pressure distribution influenced by boreholes, the mesh density between the adjacent boreholes (in the same group) is five times of that out of the adjacent boreholes. The input parameters used in the numerical model were listed in Table 1, most of which were obtained from experiments and the others chosen from an appropriate range obtained from recently published studies (An et al., 2013). In particular, the maximum drainage time is 600 d obtained by evaluating the mining speed and engineering progress.

4. Simulation results and discussion

4.1. Case A: disadvantages of drainage design without considering the influences of the inhomogeneous distributions of gas pressure and coal permeability

Fig. 4 illustrates the gas pressure (p_f) distributions after drainage 100 d and 600 d respectively. As the initial pressure and initial coal permeability were constant, 6 boreholes with different spacings were applied in the middle of the solution domain, the x-coordinate of the left-most borehole was 700 and the spacings between the adjacent boreholes from the left to the right were 15 m, 20 m, 25 m, 30 m and 50 m, respectively. It is clear that the low gas pressure zone was located around the roadway and drainage boreholes, and which expanded with the drainage time. The maximum pressure is 1.58 MPa, and the minimum pressure is 87 kPa, which is equal to the initial pressure and borehole drainage pressure respectively.

Based on the obtained numerical results of gas pressure, the reasonable spacing of boreholes was further analyzed. Fig. 5 a shows the gas pressure along a line (y = 200, x ∈ (700, 840)) varying with drainage time of 100 d, 200 d, 300 d, 400 d, 500 d and 600 d, respectively. These 6 pressure distribution lines are divided into 5 groups by the boreholes, showing a parabolic shape with different characteristics influenced by the borehole spacings. The minimum gas pressure of the 5 groups of lines is equal (87 kPa). However, the maximum gas pressure increases with the increasing spacing, and decreases with the increasing drainage time. The critical value of 0.74 MPa is an index for evaluating coal and gas outburst dangers of a coal seam, thus, whether the maximum gas pressure is lower than 0.74 MPa can be used to judge the feasibility

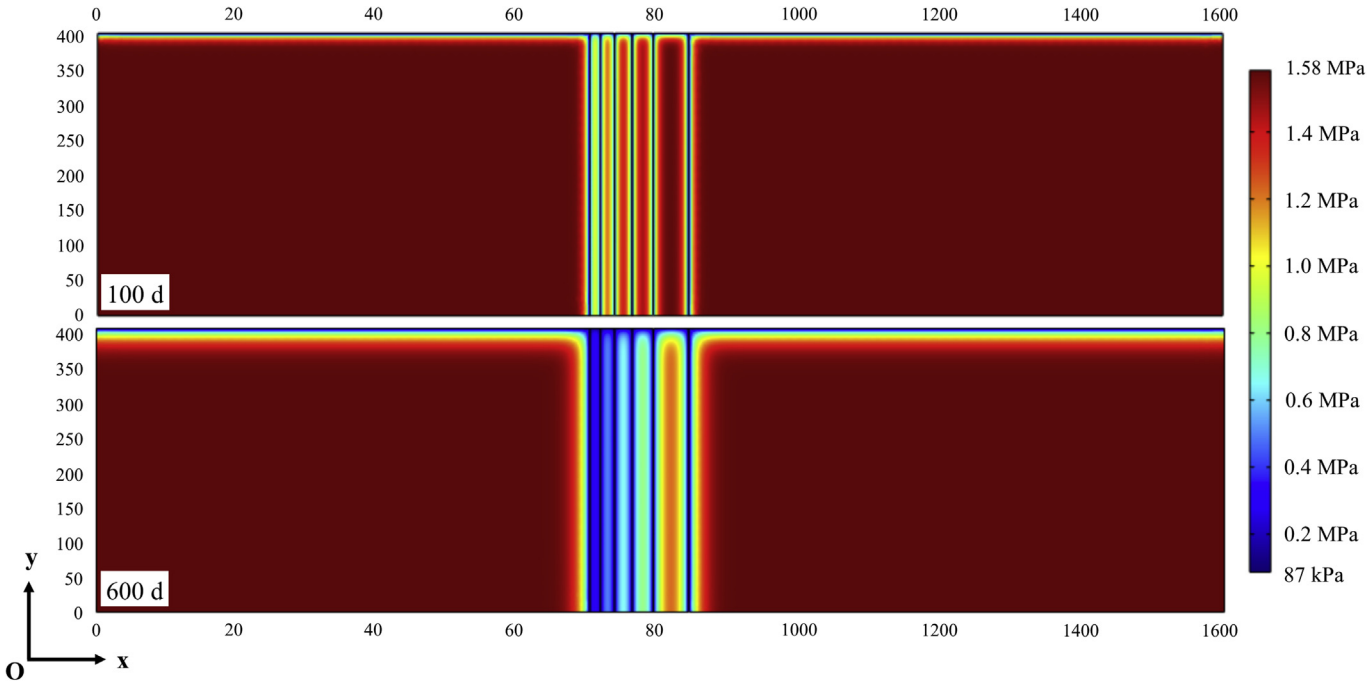

Fig. 4. Illustration of the gas pressure distributions after drainage 100 d and 600 d.

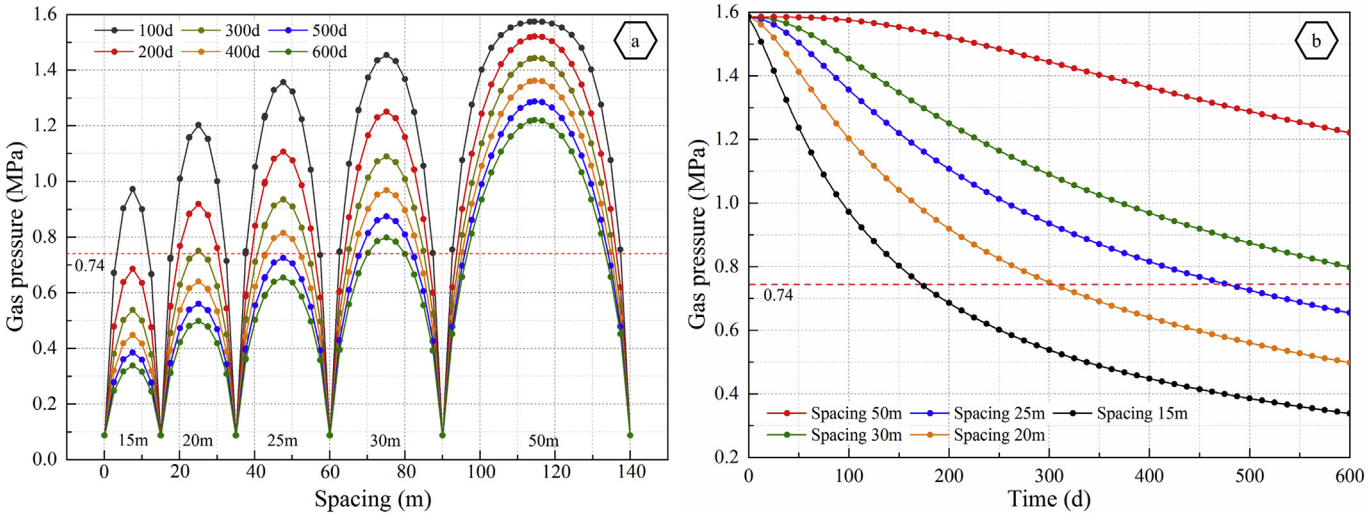

Fig. 5. Comparison of gas pressures with different borehole spacings.

of the borehole spacing. For the engineering condition discussed in this research, the drainage time is definite (600 d), thus, as shown in Fig. 5 a, it can be concluded that the borehole spacings of 15 m, 20 m and 25 m are feasible design. However, the design feasibility is only the basic requirement of the optimal design. Fig. 5 b shows the maximum gas pressures of the 5 borehole spacings varying with drainage time. The essential drainage time for spacings of 15 m, 20 and 25 m is about 170 d, 300 d, and 470 d, respectively. For these three feasible spacings, the reduction speed of the maximum gas pressure decreases with the increasing drainage time, meaning the drainage efficiency decreases with the increasing drainage time. As the drainage time is definite (600 d), shorter essential drainage time does not bring more benefits. In addition, the engineering workload for spacings of 15 m is 1.7 times more than that for spacings of 25 m. Thus, the spacing of 25 m is the most optimal design among the three feasible spacings.

Though it is clear that the optimal spacing is between 25 m and 30 m, we are going to discuss the pressure evolution by setting the borehole spacings of 25 m and 30 m with considering the inhomogeneous gas pressure and coal permeability distributions, i.e., the real gas drainage effect and disadvantages of the above obtained “optimal design” will be discussed. As shown in Figs. 6 and 12 boreholes were divided into 4 groups (named group A to group D from left to right), and the locations of the 4 groups were selected based on the initial pressure distribution characteristics. It is clear that the gas pressure distribution is quite different from that without considering the inhomogeneous gas pressure and coal permeability distributions. The maximum gas pressure is 1.62 MPa, and the minimum one is 87 kPa. For the boreholes in the same group, the gas pressure within their influenced area decreases with

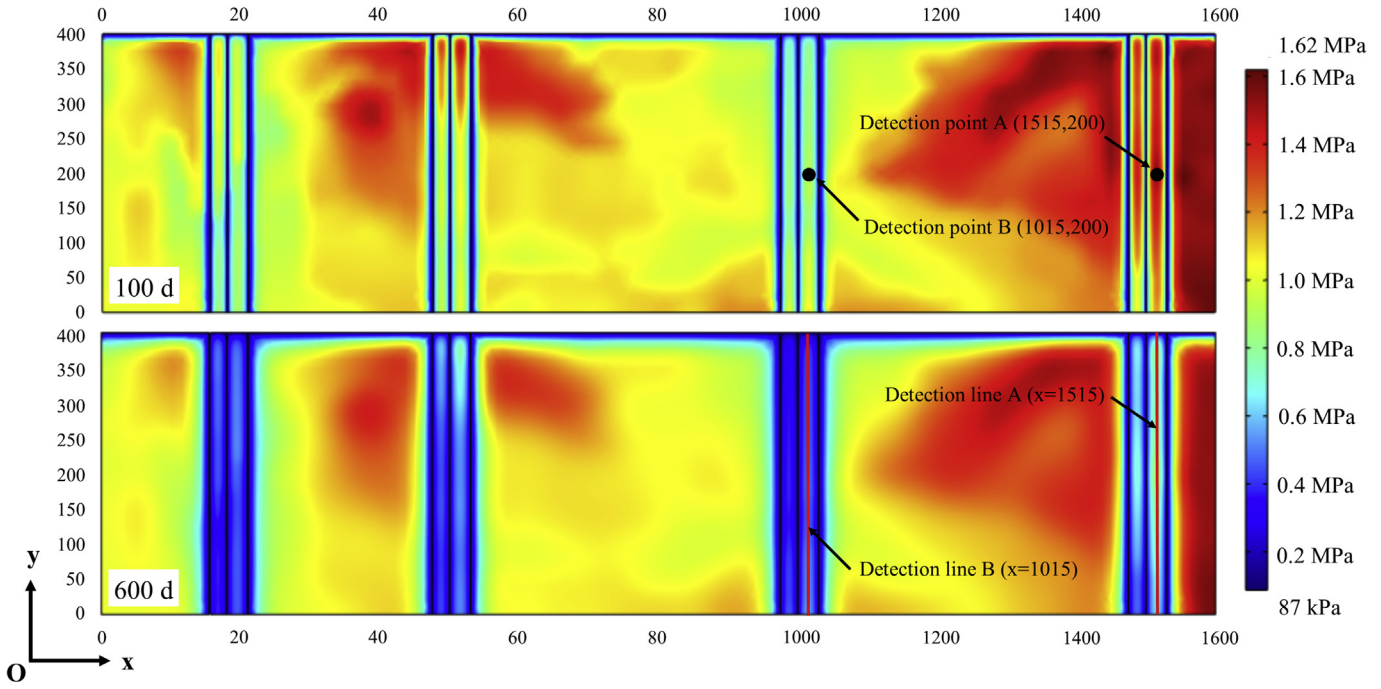

Fig. 6. Illustration of the gas pressure distributions under the practical inhomogeneous initial condition after drainage 100 d and 600 d.

the increasing drainage time and shows strong nonuniform distribution character. Under the same spacing and drainage time condition, the gas pressures within different groups of boreholes are quite different. In addition, the gas pressure of the borehole uninfluenced area also shows strong inhomogeneous distribution character.

In the following, quantitative analyses of gas drainage effect and disadvantages without considering the influences of the inhomogeneous distributions of gas pressure and coal permeability were conducted based on the gas pressure distribution data of the typical detection lines and detection points. Fig. 7 shows the pressure distributions of three detection lines after drainage 600 d, and the three detection lines are y = 200, y = 300, and y = 350, respectively. It is clear that the real drainage effect was strongly influenced by the inhomogeneous gas pressure and coal permeability distributions. The gas pressures for the 4 groups of boreholes were quite different even under the same drainage time and spacing condition. The gas pressure for the left 3 groups of boreholes decreased below 0.74 MPa no matter the spacing was 25 m or 30 m, however, the gas pressure for group D when spacing was 30 m was still higher than 0.74 MPa. For group A and group C of boreholes, the gas pressure of the 3 detection lines had little difference, however, which can not be ignored for group B and group D of boreholes. Thus, it can be concluded that the real drainage effect of the drainage design greatly deviated from the simulation result obtained without considering the inhomogeneous gas pressure and coal permeability distributions.

Further, disadvantages of drainage design without considering the influences of the inhomogeneous distributions of gas pressure and coal permeability can be discussed from two aspects: “time”

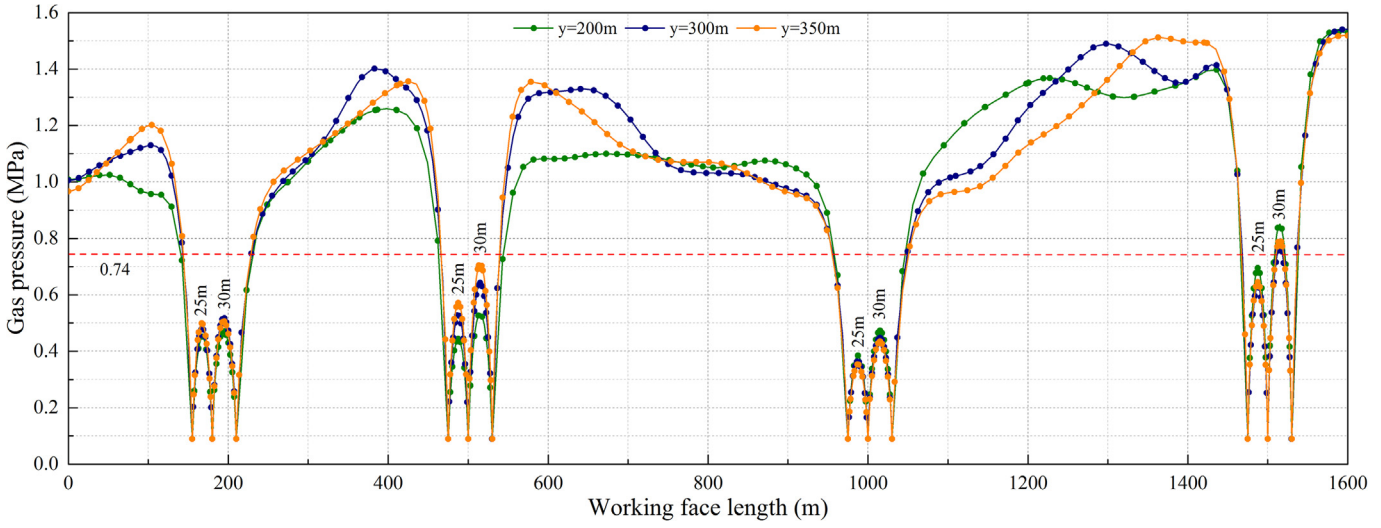

Fig. 7. Gas pressure distributions along three detection lines (y = 200, y = 300 and y = 350) after drainage 600 d.

and “space”. Fig. 8 shows the gas pressures along two detection points varying with drainage time. The two typical detection points were point A (1515, 200) and point B (1015, 200), and the former was located in the middle between two boreholes (spacing 30 m) from group D, and the later was located in the middle between two boreholes (spacing 30 m) from group C. Though the two detection points were under the same borehole spacing condition, it only needed about 210 d for the gas pressure of point B to decrease below 0.74 MPa, the gas pressure of point A was still above 0.74 MPa after drainage 600 d. As we have pointed out that shorter essential drainage time doesn't bring more benefits when the drainage time is definite (600 d), so for group C, drilling boreholes with a spacing of 30 m increased unnecessary engineering cost and it was not an optimal design. It can be concluded that gas drainage design without considering the inhomogeneous gas pressure and coal permeability distributions will increase unnecessary engineering cost.

The disadvantage induced by “space” was closely related to the mining safety. Gas pressure distributions along two detection lines which were x = 1515 (line A) and x = 1015 (line B) after drainage 100 d and 600 d were shown in Fig. 9. The two detection lines were parallel to the boreholes and point A and point B were located on line A and line B, respectively, i.e., the two detection lines were also under the same borehole spacing condition. After drainage 600 d, the gas pressure on line B was below 0.74 MPa, however, which only on the part of line A was below 0.74 MPa. According to the engineering practice, we need to evaluate and justify coal and gas outburst dangers by testing the residual gas pressure of the pre-drainage coal seam after drainage. Thus, there will be an enormous risk if the residual gas pressure test point is located in the low gas pressure area (<0.74 MPa).

From the above discussion it should be clear that, there are two main disadvantages of drainage design without considering the influences of the inhomogeneous distributions of gas pressure and coal permeability, the first one is that it will increase unnecessary engineering cost and the second one is that it may produce an enormous risk.

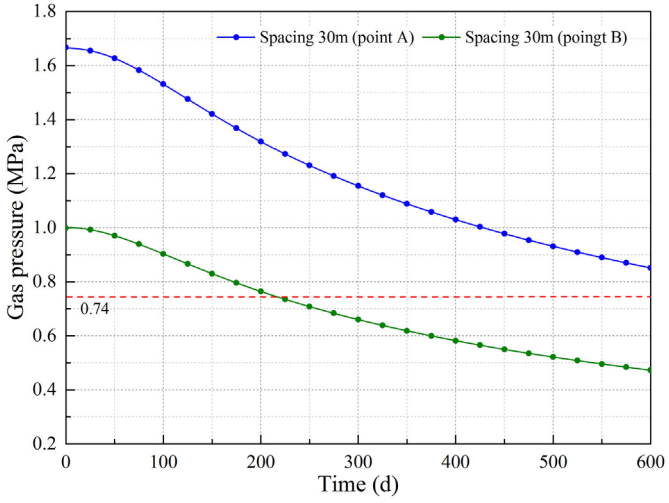

Fig. 8. Gas pressures of two detection points (A (1515, 200) and B (1015, 200)) varying with drainage time.

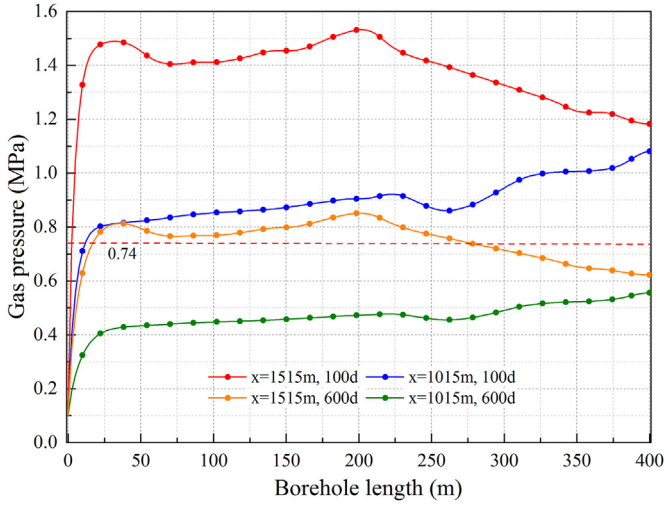

Fig. 9. Gas pressure distributions along three detection lines (x = 1515 and x = 1015) after drainage 100 d and 600 d.

4.2. Case B: how to make gas drainage design with considering the influences of the inhomogeneous distributions of gas pressure and coal permeability

The influences of the loess plateau geomorphology on gas drainage design are mainly from the inhomogeneous gas pressure and coal permeability distributions. Thus, the first stage to make gas drainage design is to evaluate the inhomogeneity of gas pressure and coal permeability. Based on the initial distribution of gas pressure and coal permeability, we made a further evaluation of the nonuniformities of them. The achieved results show that we can get a same drainage difficulty judgement of pre-drainage by using both gas pressure and coal permeability as the evaluation index, substantially simplifying the evaluation procedure. We introduce the median value of gas pressure and coal permeability as the critical value to make the partition of the pre-drainage seam. By doing this, we can divide the pre-drainage seam into several zones with lower nonuniformities of gas pressure and coal permeability within each zone.

As discussed in section 3.2, in the pre-drainage seam, the gas pressure ranges from 0.81 MPa to 1.66 MPa, and coal permeability ranges from 0.0137 mD to 0.0508 mD. The median value of gas pressure and coal permeability were set as 1.2 MPa and 0.032 mD. The logical judgement results of the initial gas pressure and coal permeability were shown in Fig. 10. When the initial gas pressure is lower than 1.2 MPa, the logical judgement result is “1”, otherwise, it is “0”. For coal permeability, when the initial value is higher than 0.032mD, the logical judgement result is “1”, otherwise, it is “0”. In particular, there was some data not equal to 1 or 0 that was located at the inside boundary between the “1” zone and the “o” zone due to the operating mechanism of COMSOL, without influencing the evaluations.

The pre-drainage seam can be divided into 6 zones based on the logical judgement results (mainly based on gas pressure logical judgement result). They were zone 1 to zone 6 from left to right. Among them, zone 1, zone 3 and zone 5 were with a lower drainage difficulty than the other three zones. The x-coordinate range of zone 1 to zone 6 was 0–60 m, 60–180 m, 180–315 m, 315–735 m, 735–1100 m and 1100–1600 m, respectively. As the former three zones were too small to influence the whole engineering cost, the drainage design of zone 1 and zone 3 was in accordance with that of zone 5, and the drainage design of zone 2 was in accordance with that of zone 4. Moreover, by comparing gas pressure distributions between zone 1, zone 3 and zone 5, it can be concluded that there was no safety risk of this simplification, which was also tenable for zone 2.

Based on the above discussion, the second stage to make gas

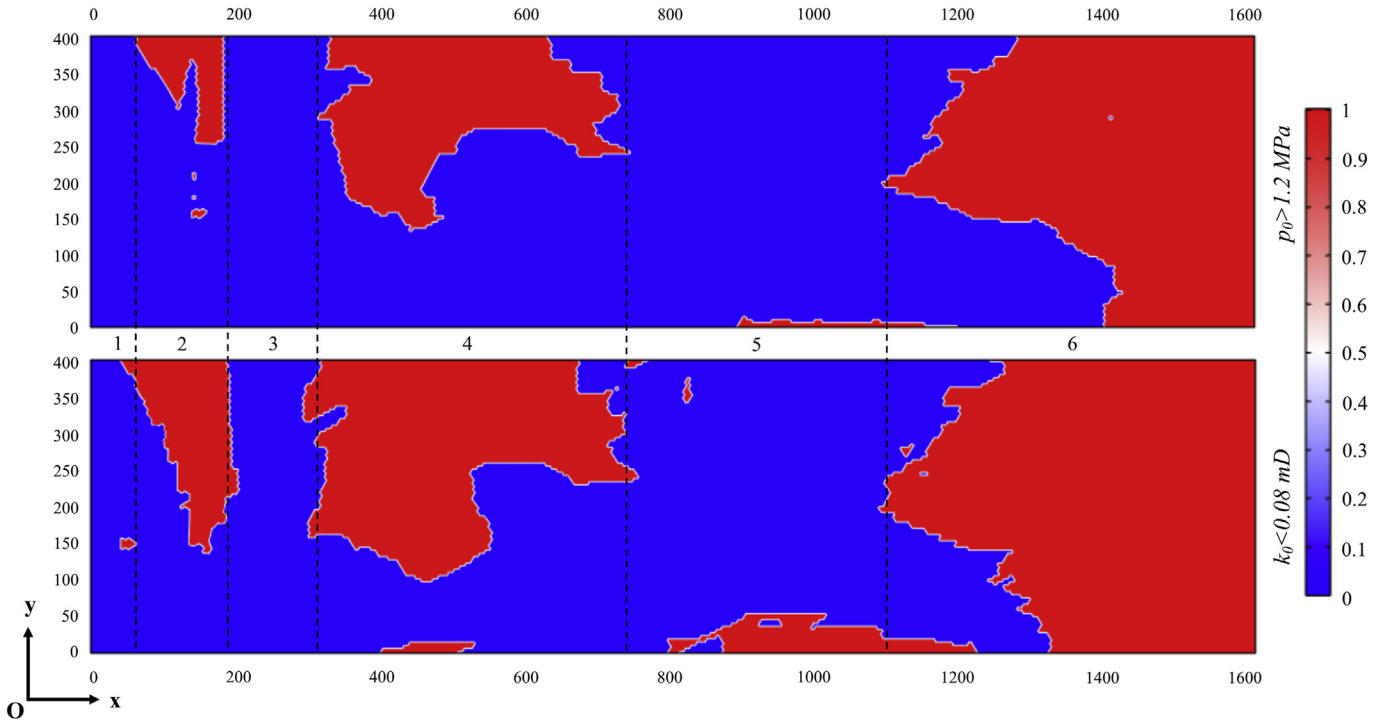

Fig. 10. Partitions of the pre-drainage seam based on the logical judgement results of the initial gas pressure and coal permeability.

drainage design is applied by conducting numerical simulations of gas pressure distributions in zone 4, zone 5 and zone 6 by setting different borehole spacings. This numerical simulation was characterized by a two-steps approach. At the first step, every 6 boreholes were set in zone 4, zone 5 and zone 6; in each zone, the borehole spacings gradually increases from left to right with a stationary added value of 5 m. For zone 4, the borehole spacings ranged from 20 m to 40 m and the x-coordinate of the leftmost borehole is 400 m; for zone 5, the borehole spacings ranged from 35 m to 55 m and the x-coordinate of the leftmost borehole is 800 m; for zone 6, the borehole spacings ranged from 15 m to 35 m and the x-coordinate of the leftmost borehole is 1400 m.

The gas pressure distributions after drainage 500 d, 550 d and 600 d, and the logical judgement results of gas pressure (with the logical judgement condition of $p < 0.74$ MPa) were shown in Fig. 11. It is clear that the borehole spacing densities in the three zones were different from each other, and gas pressure within the borehole influenced area was quite lower than the uninfluenced area after drainage more than 500 d. However, the gas pressure within borehole influenced area still shows inhomogeneous characteristic. Thus, it is needed to conduct regional logical judgement of residual gas pressure. As shown in Fig. 11, the area where the residual gas pressure is higher than 0.74 MPa decreases with the increasing drainage time within the borehole influenced area, and when it disappears, it can be concluded that the corresponding borehole spacings are feasible. Take, for example, the performance of borehole spacings were analyzed based on the logical judgement results of the residual gas pressure in zone 4. The fessible borehole spacings were 20 m and 25 m for zone 4 after drainage 500 d, and which were 20 m, 25 m, and 30 m after drainage 550 d and 600 d. As the fessible spacing increases with drainage time, it can concluded that maximum borehole spacing which is the optimal spacing may be larger than 30 m after drainage 600 d, i.e., it can be concluded that the optimal borehole spacing was between 30 m and 35 m. Based on the same analysis procedure, we obtained the optimal borehole spacing for zone 5 was between 40 m and 45 m, and for zone 6 was between 25 m and 30 m. However, the critical value of the optimal borehole spacing can not be obtained at the first step due to the lack of adequate information, the seconde step should be implemented.

At the second step, boreholes were set according to that of the first step, but the stationary added value of borehole spacing now was 1 m, i.e., the borehole spacings for zone 4 ranged from 30 m to 34 m, for zone 5 ranged from 40 m to 44 m, and for zone 6 ranged from 25 m to 29 m. Under the new conditions, the gas pressure distributions after drainage of 500 d, 550 d, and 600 d, and the logical judgement results of gas pressure (with the logical judgement condition of $p < 0.74$ MPa) were shown in Fig. 12. Take, for example, the performance of borehole spacings were also analyzed based on the logical judgement results of the residual gas pressure of zone 4. After drainage 550 d, the feasible borehole spacing was 30 m; after drainage 600 d, the feasible borehole spacings were 30 m and 31 m. Though it is possible that the optimal borehole spacing is between 31 m and 32 m, without markedly influencing the engineering cost, the optimal borehole spacing of 31 m was recommended for zone 4. Using the same analysis procedure, we recommended the optimal borehole spacings for zone 5, and zone 6 were 41 m and 27 m, respectively.

To sum up, the optimal borehole spacing of 41 m was recommended for zone 1, zone 3 and zone 5, the optimal borehole spacing of 31 m was recommended for zone 2 and zone 4, and the optimal borehole spacing of 27 m was recommended for zone 6.

Without considering the influences of the inhomogeneous distributions of gas pressure and coal permeability, about 65 boreholes are needed. However, only about 51 boreholes are needed with considering the influences of the inhomogeneous distributions of gas pressure and coal permeability, saving about 21.5% engineering cost. More important, coal and gas outburst dangers would be eliminated preferably by conducting the gas drainage design with considering the influences of the inhomogeneous distributions of gas pressure and coal permeability.

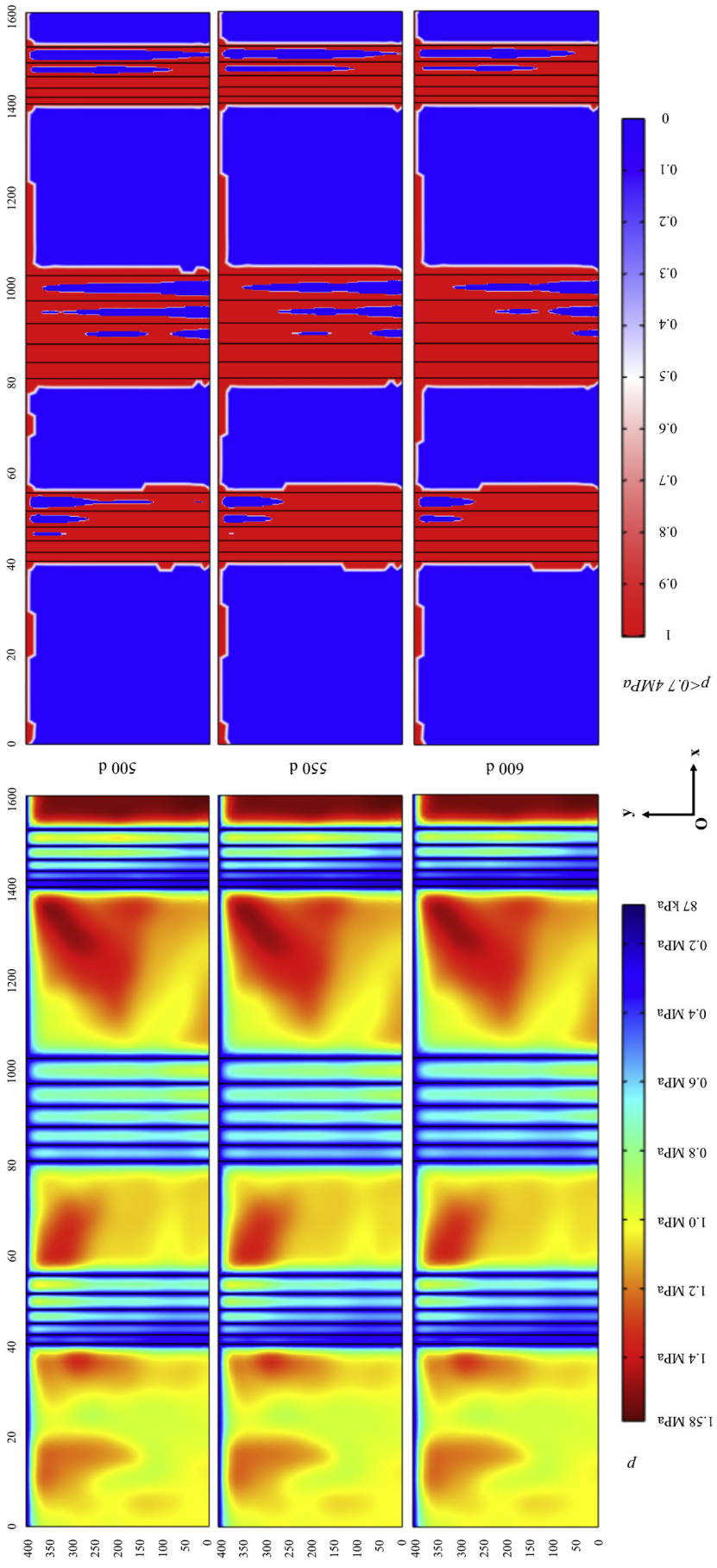

Fig. 11. Illustration of the gas pressure distributions and the corresponding logical judgement results after drainage 500 d, 550 d and 600 d (for the first step).

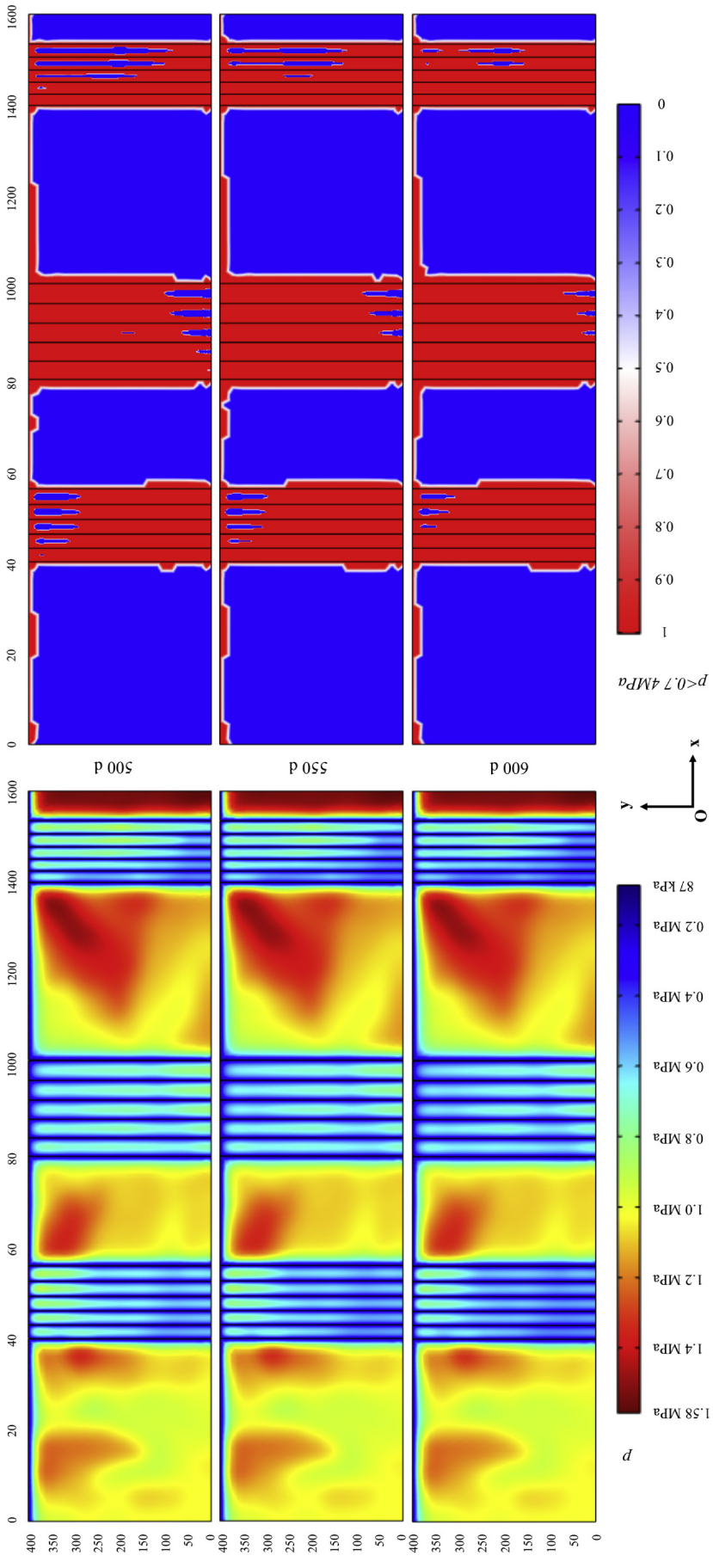

Fig. 12. Illustration of the gas pressure distributions and the corresponding logical judgement results after drainage 500 d, 550 d and 600 d (for the second step).

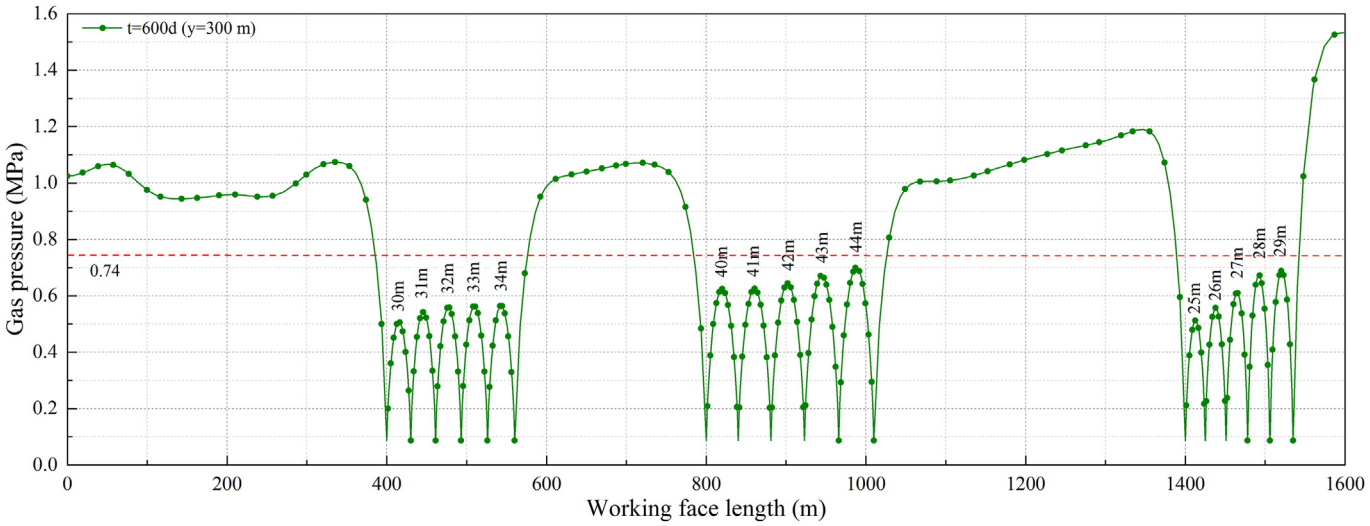

Fig. 13. Gas pressure distribution along the line y = 300 m after drainage 600 d.

It should be noted especially that the above obtained optimal borehole spacings were limited by the engineering conditions: boreholes were straight and with no branch; the drainage time was specified. As shown in Fig. 12, after drainage of 600 d, it is clear that the residual gas pressure of small areas was higher than 0.74 MPa within the borehole influenced area for all the three zones. For a clear description, the gas pressure along the line y = 300 m after drainage 600 d was extracted and shown in Fig. 13; it can be found the gas pressure was lower than 0.74 MPa for all borehole spacings. So, if the boreholes can be drilled with suitable branches, more engineering cost would be saved. Moreover, if the drilling trace can be well controlled and designed based on the numerical simulation results, another more engineering cost would be saved, which is based on the combination of gas drainage theory and borehole drilling technology and equipment. To sum up, it also suggests that with considering the influences of the loess plateau geomorphology, the analysis of borehole performance are helpful to the gas drainage technological innovations.

5. Conclusions

In this study, theoretical/numerical modeling are conducted to study the influences of the inhomogeneous distributions of gas pressure and coal permeability on gas drainage of the pre-drainage seam. Theoretical modeling is developed by fully coupling gas flow, gas diffusion, and permeability evolution. Numerical modeling is achieved by using COMSOL Multiphysics software based on the finite element method. As the influences of the loess plateau geomorphology on gas drainage are reflected in the inhomogeneous initial distributions of gas pressure and coal permeability, image recognition technology is applied to rebuilt this initial condition in two numerical case studies. Based on the work completed, the following conclusions are made:

(1) The image recognition was achieved by scaling the RGB values of the distributions of gas pressure and coal permeability in each pixel, providing the practical inhomogeneous initial condition for the numerical simulation.
(2) The borehole design with good performance obtained without considering the influences of loess plateau geomorphology, showing quite poor performance when applied to the practical conditions of the pre-drainage seam, i.e., the loess plateau geomorphology greatly influences gas drainage of the pre-drainage seam. Based on the comparisons, two main disadvantages of drainage design without considering the influences of the loess plateau geomorphology are visually revealed, including unnecessary engineering cost and enormous mining risk.
(3) The procedure of making optimal gas drainage design with considering the influences of the inhomogeneous distributions of gas pressure and coal permeability is presented. At the first stage, by comparing to the median value of gas pressure (1.2 MPa) and coal permeability (0.032 mD), the pre-drainage seam is divided into 6 zones with lower non-uniformities within each zone. At the second stage, two-steps numerical simulations are conducted to analysis the performance of different borehole spacings in different zones. Based on the two stages analysis, the optimal borehole spacings are obtained, which for zone 1, zone 3 and zone 5 is 41 m, for zone 2 and zone 4 is 31 m, and for zone 6 is 27 m, saving about 21.5% engineering cost compared to the design without considering the influences of the inhomogeneous distributions of gas pressure and coal permeability.

The simulation results in this work reveal that the optimal gas drainage design should be made based on a comprehensive evaluation of engineering conditions, which are also helpful to the gas drainage technological innovations. More additional works are highly required in the future to develop an accessible combination of gas drainage theory and borehole drilling technology and equipment.

Acknowledgements

The authors are grateful to the financial support from a project funded by Natural Science Foundation of Jiangsu Province (No. BK20160253), China Postdoctoral Science Foundation (No. 2016M590519), the State Key Laboratory of Coal Resources and Safe Mining (No. SKLCRSM16KFB01), the Fundamental Research Funds for the Central Universities (No.2013RC05), Natural Science Foundation for the Youth of China (No. 51604174) and a project funded by the Priority Academic Program Development of Jiangsu Higher Education Institutions and the Fundamental Research Funds for the Central Universities (No. 2013QNA03).

Nomenclature

p_f	pressure in the fractures, MPa
p_m	pressure in the matrix blocks, MPa
Q_m	gas exchange rate per volume of coal matrix, kg/(m^3·s)
c_m	concentration of gas in the matrix blocks, kg/m^3
c_f	concentration of gas in the fractures, kg/m^3
τ	sorption time, s
D	gas diffusion coefficient, m^2/s
σ_c	coal matrix block shape factor, m^{-2}
M_c	molar mass of methane, kg/mol
R	universal gas content, J/(mol·K)
T	temperature, K
m	quantify of adsorbed gas and free gas per volume of coal matrix blocks, kg/m^3
t	time, s
V_L	maximum adsorption capacity of coal, kg/m^3
P_L	Langmuir pressure constant, Pa
V_M	molar volume of methane under standard condition, m^3/mol
ρ_c	coal density, kg/m^3
ϕ_m	coal matrix porosity, %
ϕ_f	fracture porosity, %
ρ_g	gas density, kg/m^3
V	gas velocity in fractures, m/s
k	coal permeability, mD
μ	methane viscosity, Pa·s
σ_{ij}^e	effective stress, MPa
σ_{ij}	total stress, MPa
δ_{ij}	Kronecker delta tensor
β_f	effective stress coefficient for fractures
β_m	effective stress coefficient for coal matrix blocks
K	bulk modulus of coal, MPa
K_m	bulk modulus of the coal grains, MPa
K_s	bulk modulus of the coal skeleton, MPa
E	Young's modulus of the coal, MPa
E_m	Young's modulus of the coal grains, MPa
υ	Poisson's ratio of the coal
ε_{ij}	component of the total strain tensor
u_i	component of the displacement in the i-direction
F_i	component of the body force in the i-direction
G	shear modulus of coal, MPa
ε_s	sorption-induced volumetric strain
ε_L	Langmuir volumetric strain
k_0	initial coal permeability, mD
ϕ_{f0}	initial fracture porosity, %
ε_p	pore volumetric strain
ε_g	grain volumetric strain
M	constrained axial modulus, MPa
p_{f0}	initial pressure in the fractures, MPa
p_{m0}	initial pressure in the matrix blocks, MPa
p_c	given constant pressure on the boundaries, MPa
$\vec{n}$	outward unit normal vector on the boundary
Ω	subdomain on which the balances are performed
$\partial\Omega$	boundaries of the subdomain

References

An, F.-h., Cheng, Y.-p., Wang, L., Li, W., 2013. A numerical model for outburst including the effect of adsorbed gas on coal deformation and mechanical properties. Comput. Geotechnics 54, 222–231.

Chen, D., Pan, Z., Liu, J., Connell, L.D., 2013. An improved relative permeability model for coal reservoirs. Int. J. Coal Geol. 109, 45–57.

Clarkson, C.R., McGovern, J.M., 2005. Optimization of CBM reservoir exploration and development strategies through integration of simulation and economics. SPE Reserv. Eval. Eng. 8, 502–519.

Detournay, E., Cheng, A.H.-D., 1993. Fundamentals of Poroelasticity, Vol 1.

Gilman, A., Beckie, R., 2000. Flow of coal-bed methane to a gallery. Transp. porous media 41, 1–16.

Hassanizadeh, S.M., 1986. Derivation of basic equations of mass transport in porous media, Part 2. Generalized Darcy's and Fick's laws. Adv. Water Resour. 9, 207–222.

Karacan, C.Ö., Ruiz, F.A., Cotè, M., Phipps, S., 2011. Coal mine methane: a review of capture and utilization practices with benefits to mining safety and to greenhouse gas reduction. Int. J. Coal Geol. 86, 121–156.

King, G.R., Ertekin, T., Schwerer, F.C., 1986. Numerical simulation of the transient behavior of coal-seam degasification wells. SPE Form. Eval. 1, 165–183.

Kriz, I., Pultr, A., 2013. Multivariable differential calculus. In: Introduction to Mathematical Analysis. Springer, pp. 65–95.

Liu, Q., Cheng, Y., 2014. Measurement of pressure drop in drainage boreholes and its effects on the performance of coal seam gas extraction: a case study in the Jiulishan Mine with strong coal and gas outburst dangers. Nat. hazards 71, 1475–1493.

Liu, Q., Cheng, Y., Yuan, L., Tong, B., Kong, S., Zhang, R., 2014. CMM capture engineering challenges and characteristics of in-situ stress distribution in deep level of Huainan coalfield. J. Nat. Gas Sci. Eng. 20, 328–336.

Liu, Q., Cheng, Y., Zhou, H., Guo, P., An, F., Chen, H., 2015. A mathematical model of coupled gas flow and coal deformation with gas diffusion and Klinkenberg effects. Rock Mech. Rock Eng. 48, 1163–1180.

Liu, Q., Cheng, Y., Haifeng, W., Hongxing, Z., Liang, W., Wei, L., Hongyong, L., 2015. Numerical assessment of the effect of equilibration time on coal permeability evolution characteristics. Fuel 140, 81–89.

Manik, J., Ertekin, T., Kohler, T., 2000. Development and validation of a compositional coalbed simulator. In: Canadian International Petroleum Conference. Petroleum Society of Canada.

Mian, C., Zhida, C., 1999. Effective stress laws for multi-porosity media. Appl. Math. Mech. 20, 1207–1213.

Mora, C., Wattenbarger, R., 2009. Analysis and verification of dual porosity and CBM shape factors. J. Can. Petrol. Technol. 48, 17–21.

Multiphysics, C., 2015. COMSOL multiphysics reference manual (version 5.2). In: Comsol, p. 269.

I. Palmer, J. Mansoori, How permeability depends on stress and pore pressure in coalbeds: a new model, in: SPE Annual Technical Conference and Exhibition, 1996.

Shi, J.Q., Durucan, S., 2003. Gas storage and flow in coalbed reservoirs: implementation of a bidisperse pore model for gas diffusion in coal matrix. In: SPE Annual Technical Conference and Exhibition. Society of Petroleum Engineers.

Shi, H., Shao, M., 2000. Soil and water loss from the Loess Plateau in China. J. Arid Environ. 45, 9–20.

Shirazian, S., Pishnamazi, M., Rezakazemi, M., Nouri, A., Jafari, M., Noroozi, S., Marjani, A., 2012. Implementation of the finite element method for simulation of mass transfer in membrane contactors. Chem. Eng. Technol. 35, 1077–1084.

Thararoop, P., Karpyn, Z.T., Ertekin, T., 2012. Development of a multi-mechanistic, dual-porosity, dual-permeability, numerical flow model for coalbed methane reservoirs. J. Nat. Gas Sci. Eng. 8, 121–131.

Valliappan, S., Zhang, W., 1996. Numerical modelling of methane gas migration in dry coal seams. Int. J. Numer. Anal. methods geomechanics 20, 571–593.

Wang, J., Kabir, A., Liu, J., Chen, Z., 2012. Effects of non-Darcy flow on the performance of coal seam gas wells. Int. J. Coal Geol. 93, 62–74.

Wei, X.R., Wang, G.X., Massarotto, P., Golding, S.D., Rudolph, V., 2007. A review on recent advances in the numerical simulation for coalbed-methane-recovery process. SPE Reserv. Eval. Eng. 10, 657–666.

Yang, T., Chen, S., Zhu, W., Liu, H., Huo, Z., Jiang, W., 2010. Coupled model of gas-solid in coal seams based on dynamic process of pressure relief and gas drainage. Rock Soil Mech. 31, 2247–2252.

Yanwei, L., Qian, W., Wenxue, C., Mingju, L., Mitri, H., 2016. Enhanced coalbed gas drainage based on hydraulic flush from floor tunnels in coal mines. Int. J. Min. Reclam. Environ. 30, 37–47.

Ye, Z., Chen, D., Wang, J., 2014. Evaluation of the non-Darcy effect in coalbed methane production. Fuel 121, 1–10.

Zhang, J., Roegiers, J., Bai, M., 2004. Dual-porosity elastoplastic analyses of non-isothermal one-dimensional consolidation. Geotech. Geol. Eng. 22, 589–610.

Zhao, G., Mu, X., Wen, Z., Wang, F., Gao, P., 2013. Soil erosion, conservation, and eco-environment changes in the Loess Plateau of China. Land Degrad. Dev. 24, 499–510.

Zhu, W., Wei, C., Liu, J., Qu, H., Elsworth, D., 2011. A model of coal–gas interaction under variable temperatures. Int. J. Coal Geol. 86, 213–221.

Zuber, M., Sawyer, W., Schraufnagel, R., Kuuskraa, V., 1987. The use of simulation and history matching to determine critical coalbed methane reservoir properties. In: Low Permeability Reservoirs Symposium.